

1 **The use of radiocarbon ^{14}C to constrain carbon dynamics in the soil module**
2 **of the land surface model ORCHIDEE (SVN r5165)**
3
4

5 **Marwa Tifafi¹, Marta Camino-Serrano^{2,3}, Christine Hatté¹, Hector Morras⁴, Lucas**
6 **Moretti⁵, Sebastián Barbaro⁵, Sophie Cornu⁶, Bertrand Guenet¹**

7
8 ¹Laboratoire des Sciences du Climat et de l'Environnement, LSCE/IPSL, CEA-CNRS-UVSQ,
9 Université Paris-Saclay, F-91191 Gif-sur-Yvette, France.

10 ²CREAF, Cerdanyola del Vallès, 08193, Catalonia, Spain

11 ³CSIC, Global Ecology Unit CREAM-CSIC-UAB, Bellaterra 08193, Catalonia, Spain

12 ⁴INTA-CIRN, Instituto de Suelos, 1712 Castelar, Buenos Aires, Argentina

13 ⁵INTA-EEA Cerro Azul, 3313 Cerro Azul, Misiones, Argentina

14 ⁶Aix Marseille Univ, CNRS, IRD, INRA, Coll France, CEREGE, Aix-en-Provence, France

15
16 Corresponding authors: Marwa Tifafi (marwa.tifafi@lsce.ipsl.fr)
17

18 **Abstract.** Despite the importance of soil as a large component of the terrestrial ecosystems,
19 the soil compartments are not well represented in the Land Surface Models (LSMs). Indeed,
20 soils in current LSMs are generally represented based on a very simplified schema that can
21 induce a misrepresentation of the deep dynamics of soil carbon. Here, we present a new
22 version of the Institut Pierre Simon Laplace (IPSL) Land Surface Model called ORCHIDEE-
23 SOM (ORganizing Carbon and Hydrology in Dynamic EcosystEms-Soil Organic Matter),
24 incorporating the ^{14}C dynamic in the soil. ORCHIDEE-SOM first simulates soil carbon
25 dynamics for different layers, down to 2 m depth. Second, concentration of dissolved organic
26 carbon and its transport are modeled. Finally, soil organic carbon decomposition is considered
27 taking into account the priming effect.

28 After implementing ^{14}C in the soil module of the model, we evaluated model outputs against
29 observations of soil organic carbon and modern ^{14}C fraction ($F^{14}\text{C}$) for different sites with
30 different characteristics. The model managed to reproduce the soil organic carbon stocks and
31 the $F^{14}\text{C}$ along the vertical profiles for the sites examined. However, an overestimation of the
32 total carbon stock was noted, primarily on the surface layer. Due to ^{14}C , it is possible to probe
33 carbon age in the soil, which was found to underestimated. Thereafter, two different tests on
34 this new version have been established. The first was to increase carbon residence time of the
35 passive pool and decrease the flux from the slow pool to the passive pool. The second was to
36 establish an equation of diffusion, initially constant throughout the profile, making it vary
37 exponentially as a function of depth. The first modifications did not improve the capacity of
38 the model to reproduce observations whereas the second test improved both estimation of
39 surface soil carbon stock as well as soil carbon age. This demonstrates that we should focus
40 more on vertical variation of soil parameters as a function of depth, in order to upgrade the
41 representation of global carbon cycle in LSMs, thereby helping to improve predictions of the
42 of soil organic carbon to environmental changes.

43 **1 Introduction**

44 The complexity of the mechanisms involved in controlling soil activity (Jastrow et al., 2007)
45 and therefore the carbon flux from the soil to the atmosphere makes predicting the response of
46 these systems to climate change extremely complex. Thus our ability to predict future changes
47 in carbon stocks in soils using global climate models is currently heavily criticized (Todd-
48 Brown et al., 2013; Wieder et al., 2013). Indeed, Earth System Models (ESMs) are
49 increasingly used today in order to predict the future evolution of the climate. For instance,
50 results of a set of ESMs are taken into account within the Intergovernmental Panel on Climate
51 Change (IPCC) (Taylor et al., 2012) for assessment of the impacts of climate change and
52 design of mitigation strategies. Hence, their predictions need to be as accurate as possible.
53 These models represent the physical, chemical and biological processes within and between
54 the atmosphere, ocean and terrestrial biosphere. They allow us to follow and understand both
55 the effect of the climate on carbon storage and vice versa. However, ESMs are continuously
56 under development and some key processes in the global carbon cycle are still missing or not
57 represented with the necessary details. One of the components of an ESM is the land surface
58 model (LSM). This component primarily manages the carbon cycle, energy and water on land
59 and simulates the carbon exchange between the land surface and the atmosphere, namely the
60 gross primary production (GPP), the autotrophic and heterotrophic respiration.

61 Despite the importance of soils as a large component of the global carbon storage, soil
62 compartments are not well represented in LSMs (Todd-Brown et al., 2013). Indeed, carbon
63 dynamics in soil described in LSMs are based on the “Century” (Parton et al., 1987) or
64 Roth-C models (Coleman et al., 1997) where soil carbon is represented as several pools with
65 different turnover rates for each pool. Carbon is decomposed in each pool, one part of which
66 is then transferred from one pool to another and the other part is lost through heterotrophic
67 respiration. In addition, soils are generally represented as a single-layer box in LSMs that do
68 not take into account the evolution and variation of soil organic processes as a function of
69 depth (Todd-Brown et al., 2013).

70 One way to reconcile this simplified representation of carbon dynamics of the models with the
71 complexity of the data collected in the field is to integrate isotopic tracers into the models
72 themselves and thus facilitate the comparison between model outputs and data (He et al.,
73 2016). Moreover, thanks to an additive constraints on the model structure, this may improve
74 the model performances. For instance, radiocarbon is an important tool for studying the
75 dynamics of soil organic matter (Trumbore, 2000). Indeed, ^{14}C data acquired from soil
76 organic matter provide complementary information on the dynamics (temporal dimension) of
77 soil organic matter. This tracer has the major advantage of being integrator of carbon
78 dynamics on long time scales (a few decades to several centuries). It is therefore a very
79 powerful tool to constrain conceptual schemes that may not be directly compared to variables
80 measured in the field (Elliott et al., 1996). Different authors have already successfully
81 implemented radiocarbon in soil models and were able to clearly show that the introduction of
82 pools with turnover time of thousands of year were unnecessary to fit radiocarbon data
83 (Ahrens et al., 2015) whereas Braakhekke et al., (2014) showed that after a reparameterization
84 of the models based on radiocarbon data the prediction of their model was quite different with
85 more carbon in top soil and less in deep soil compared to the model without radiocarbon.

86 Radiocarbon is produced naturally at a constant rate in the upper atmosphere through
87 bombardment of cosmic rays. It thus provides information on the dynamics of organic matter
88 that has been stabilized by interaction with mineral surfaces and stored long enough for
89 significant radioactive decay (Trumbore, 2000), as the half-life of ^{14}C is about 5730 years. We
90 must also take into account radiocarbon produced during atmospheric tests of thermonuclear
91 weapons in the early sixties (Delibrias et al., 1964; Hua et al., 2013). Atmospheric bomb
92 testing in the late 1950s and early 1960s lead to an abrupt doubling of atmospheric ^{14}C
93 concentration in a span of 2-3 years. Through exchange with ocean and terrestrial reservoirs,
94 it has decreased but still remains above the natural background. As with any other carbon
95 isotopes, this ^{14}C was metabolized by the vegetation and transferred to soil. By measuring ^{14}C
96 activity of a soil sample, it is possible to evaluate the amount of carbon introduced into the
97 soil since the 1960s (Balesdent and Guillet, 1982; Scharpenseel and Schiffmann, 1977).

98 In this study, we present a new version of the IPSL-Land Surface Model called ORCHIDEE-
99 SOM incorporating ^{14}C dynamics in the soil. Thanks to this tracer, we can evaluate the SOC
100 dynamics, in particular by looking at the ^{14}C peak produced by atmospheric weapons testing
101 and observed in the soils at four different sites having different biomes.

102

103 **2 Materials and methods**

104 **2.1 ORCHIDEE-SOM overview**

105 ORCHIDEE is the Land Surface Model of the IPSL Earth System Model (Krinner et al.,
106 2005). It is composed of three different modules. First, SECHIBA (Ducoudré et al., 1993;
107 Rosnay and Polcher, 1998), the surface-vegetation-atmosphere transfer scheme, describes the
108 soil water budget and energy and water exchanges. The time step of this module is 30 min.
109 Second, the module of the vegetation dynamics has been taken from the dynamic global
110 vegetation model LPJ (Sitch et al., 2003). The time step of this module is one year. Finally,
111 the STOMATE (Saclay Toulouse Orsay Model for the Analysis of Terrestrial Ecosystems)
112 module simulates vegetation phenology and carbon dynamics with a time step of one day.

113 ORCHIDEE can be run coupled to a global circulation model where the boundary conditions
114 of the model are provided by the atmospheric modules (temperature, precipitation,
115 atmospheric CO_2 concentration, etc.). In return ORCHIDEE provides the land surface carbon,
116 energy and water fluxes. However, since our study focuses on changes in the land surface
117 rather than on the interaction with climate, we ran ORCHIDEE in the off-line configuration.
118 In this case, atmospheric conditions such as temperature, humidity and wind are read from a
119 meteorological dataset. The climate data CRUNCEP used for our study (6-hourly climate data
120 over several years) were obtained from the combination of two existing datasets: the Climate
121 Research Unit (CRU) (Mitchell et al., 2004) and the National Centers for Environmental
122 Prediction (NCEP) (Kalnay et al., 1996).

123 Our starting point is a ORCHIDEE-SOM version based on the SVN r3340 (Krinner et al.,
124 2005), which is presented in detail in Camino-Serrano et al. (2017). Figure 1 represents how
125 the soil is described in this new version. Indeed, the major particularity of ORCHIDEE-SOM
126 is that it simulates the dynamics of soil carbon for eleven layers from the surface to two

127 meters depth. First, litter is divided into four pools: metabolic or structural litter pools which
 128 can be found below or aboveground. Only the belowground litter is modeled on eleven levels,
 129 from surface to 2 m depth, as the aboveground litter layer has a fixed thickness of 10 mm.
 130 Second, SOC is divided into three pools (active, passive and slow), following Parton et al.
 131 (1988), which differ in their turnover rates and which are discretized into 11 layers up to a
 132 depth of two meters. Then, dissolved organic carbon (DOC) is represented as two pools and
 133 also discretized over 11 layers up to a depth of two meters: labile DOC has a high
 134 decomposition rate and recalcitrant DOC has a low decomposition rate (Camino-Serrano et
 135 al., 2018). Finally, another particularity of this version of ORCHIDEE-SOM is that the SOC
 136 decomposition is modified to account for the priming effect following Guenet et al. (2016).
 137 Briefly, priming is described following equation 1.

$$138 \frac{\partial SOC_{i,z}}{\partial t} = DOC_{Recycled,i,j}(t) - k_{SOC,i} \times (1 - e^{-c \times LOC_z(t)}) \times SOC(t)_{i,z} \times \theta(t) \times \tau(t) \quad (1)$$

139 with $DOC_{recycled}$ being the unrespired DOC that is redistributed into the pool i considered for
 140 each soil layer z in $g\ C\ m^{-2}\ days^{-1}$, k_{SOC} being a SOC decomposition rate constant ($days^{-1}$), and
 141 LOC being the stock of labile organic C defined as the sum of the C pools with a higher
 142 decomposition rate than the pool considered within each soil layer z . We therefore considered
 143 that for the active carbon pool LOC is the litter and DOC, but for the slow carbon pool LOC
 144 is the sum of the litter, DOC and so on. Finally, c is a parameter controlling the impact of the
 145 LOC pool on the SOC mineralization rate, i.e., the priming effect. The equation was
 146 parameterized based on soil incubations data and evaluated over litter manipulation
 147 experiments (Guenet et al. 2016).

148 Since the soil profile is divided into 11 layers, SOC and DOC transport following the
 149 diffusion must also be described. SOC diffusion is actually a representation of bioturbation
 150 processes (animal and plant activity), whereas DOC relies more on non-biological diffusion.
 151 Both diffuse through concentration gradients.

152 This is represented using the Fick's law (Braakhekke et al., 2011; Elzein and Balesdent, 1995;
 153 O'Brien and Stout, 1978; Wynn et al., 2005):

$$154 F_D = -D * \frac{\partial^2 C}{\partial z^2} \quad (2)$$

155 Where F_D is the flux of carbon transported by diffusion in $g\ C\ m^{-3}\ day^{-1}$, D is the diffusion
 156 coefficient ($m^2\ day^{-1}$) and C is the amount of carbon in the pool (DOC or SOC) subject to
 157 transport ($g\ C\ m^{-3}$). The diffusion coefficient is assumed to be constant across the soil profile
 158 in ORCHIDEE-SOM but the diffusion parameters (D) used in the equations for SOC and
 159 DOC can differ. All the transport processes goes up to two meters, corresponding to the soil
 160 depth fixed in the model. For DOC, at two meters the DOC can be exported through drainage.

161 2.2 ORCHIDEE-SOM-¹⁴C

162 In ORCHIDEE-SOM, the different compartments (soil carbon input, litter, SOC, DOC and
 163 heterotrophic respiration) are presented as a matrix with a single dimension referring to the
 164 total carbon. In order to introduce the ¹⁴C, a new dimension has been added to all the
 165 variables cited above. Thus, all processes that apply to the total soil carbon are now also
 166 represented for ¹⁴C. We label this new version including ¹⁴C as ORCHIDEE-SOM-¹⁴C.

167 Several ways of reporting ^{14}C activity levels are available. We chose to use the *fraction*
 168 *modern*, with the $F^{14}\text{C}$ symbol as advocated by Reimer et al. (2004) rather than absolute
 169 concentration of ^{14}C (reported as Bq).

$$170 \quad F^{14}\text{C} = \left(\frac{A_S}{0.95 A_{OX1}} \right) * \left(\frac{0.975}{0.981} \right)^2 * \left[\frac{\left(1 + \delta^{13}\text{C}_{OX1} / 1000 \right)}{\left(1 + \delta^{13}\text{C}_S / 1000 \right)} \right]^2 \quad (3)$$

171 with $A = ^{14}\text{C}/^{12}\text{C}$, S for sample, OX1 for Oxalic Acid 1, the ^{14}C international standard.
 172 $F^{14}\text{C}$ is twice normalized: i) it takes into account isotopic fractionation by being normalized to
 173 a $\delta^{13}\text{C} = -25\%$, and ii) it corresponds to a deviation towards an international standard (i.e.
 174 95% of OX1 as measured in 1950 – (Stuiver and Polach, 1977)). By propagating $F^{14}\text{C}$ from
 175 atmosphere at the origin of vegetal photosynthesis to soil respired CO_2 , there is no need to
 176 focus on ^{13}C isotopic fractionation all along the organic matter mineralization with $F^{14}\text{C}$.

177 To make the reading of the paper easier, we will further express $F^{14}\text{C}$ as $F^{14}\text{C} = A_{\text{sample}}/A_{\text{ref}}$
 178 with A_{sample} being the A of the measured (or modeled) data and A_{ref} an international reference.
 179 Normalizations are included in A_{ref} and $F^{14}\text{C}$ will be written as F^{14} to simplify notation
 180 involving superscripts and subscripts.

181 Since we focus on SOC dynamics, we did not include the ^{14}C in the plants but did include ^{14}C
 182 in the litter. The ^{14}C -litter is obtained by multiplying the atmospheric value by the total carbon
 183 in the litter:

$$184 \quad \text{Litter } (^{14}\text{C}) = F_{\text{atm}}^{14} * \text{Litter } (\text{C}) \quad (4)$$

185 where F_{atm}^{14} is the $F^{14}\text{C}$ of atmosphere at the time of leaf growth (figure 2).

186 Thus, from the litter, all processes defined in section 2.1 that apply to total soil carbon are also
 187 represented for ^{14}C .

188 We also take into account the radioactive decay of ^{14}C . For that, we calculate the amount of
 189 ^{14}C as follow:

$$190 \quad ^{14}\text{C} = ^{14}\text{C} - K_{\text{decrease}} * ^{14}\text{C} \quad (5)$$

191 Where k_{decrease} is the radioactive decay constant ($= \text{Ln}2/5730$) (Godwin, 1962)

192 The $F^{14}\text{C}$ of the soil is then calculated back for carbon, per pool:

$$193 \quad F_{\text{Pool},z}^{14} = \frac{{}^{14}\text{C}_{\text{Pool},z}}{\text{C}_{\text{Pool},z}} \quad (6)$$

194 with *pool* representing the active, slow or passive pool.

195 Finally, we calculate a mean $F^{14}\text{C}$ value per soil layer, according to the depth:

$$196 \quad F_{\text{Mean},z}^{14} = \frac{F_{\text{active},z}^{14} * {}^{14}\text{C}_{\text{active},z} + F_{\text{slow},z}^{14} * {}^{14}\text{C}_{\text{slow},z} + F_{\text{passive},z}^{14} * {}^{14}\text{C}_{\text{passive},z}}{{}^{14}\text{C}_{\text{active},z} + {}^{14}\text{C}_{\text{slow},z} + {}^{14}\text{C}_{\text{passive},z}} \quad (7)$$

197

198 2.3 Site descriptions

199 2.3.1 French sites

200 Two Luvisol (WRB, 2006) profiles located in the northern France were selected: the
201 Feucherolles and Mons sites. In Mons (49.87°N, 3.03°E), Luvisol, the soils sit under
202 grassland, and are developed from several meters of loess and therefore well drained. The
203 mean annual air temperature is 11°C and the annual precipitation is about 680 mm
204 (Keyvanshokouhi et al., 2016). In Feucherolles (48.9°N, 1.97°E), the soil sits under oak forest
205 and clay and gritstone deposits are found at approximately 1.5 m depth. The mean annual air
206 temperature is 11.2°C and the annual precipitation is about 660 mm (Keyvanshokouhi et al.,
207 2016). Both soils are neutral to slightly acidic and are characterized by the presence of a clay
208 accumulation Bt horizon with clay content reaching 30 % for Feucherolles and 27 % for
209 Mons, while the upper horizons are poorer in clay (17 % for Feucherolles and 20% for Mons).

210 The ¹⁴C data from the soils of both sites were obtained after chemical treatment done at
211 Laboratoire des Sciences du Climat et de l'Environnement (LSCE) using a protocol adapted
212 to achieve carbonate leaching without any loss of organic carbon; ¹⁴C activity was measured
213 by AMS at the French Laboratoire de mesure du ¹⁴C (LMC14) facility (Cottureau et al.,
214 2007). Details on measurements and sampling can be found in Jagercikova et al., (2017)

215 2.3.2 Congo site

216 The studied site is located in Kissoko (4.35°S, 11.75°E). It belongs to the SOERE F-ORE-T
217 (Site de l'Observatoire de Recherche en Environnement sur le Fonctionnement des
218 écosystèmes fORESTiers) field observation sites of Pointe Noire, Republic of Congo. The
219 mean annual air temperature is about 25°C with low seasonal variation (± 5°C), and average
220 annual precipitation of 1400mm, and a dry season between June and September. The deep
221 acidic sandy soil is a ferralic Arenosol (WRB, 2006). The soil is characterized by a sand
222 content larger than 90% (Laclau et al., 2000). A soil profile was taken under native savanna
223 vegetation dominated by C4 plants (Epron et al., 2009). The soil was sampled in May 2014 at
224 different depths: 0-5cm, 5-10cm, 10-15cm, 15-20cm, 20-30cm, 30-40cm, 40-50cm, 50-60cm,
225 60-80cm, 80-100cm, 100-120cm. All samples were crushed and air-dried. Once in the
226 laboratory, they were homogenized, crushed, randomly subsampled and sieved at 200µm.
227 Then ¹⁴C measurements were made the same way as the two French sites, using the LSCE
228 chemical treatment and the French LMC14 facility following recommendations by Cottureau
229 et al., (2007).

230 2.3.3 Argentina site

231 The Province of Misiones is located in northeastern Argentina. The climate is subtropical
232 humid without a dry season, an annual mean temperature of 20°C and 1850mm of mean
233 annual rainfall (Morrás et al., 2009). The profile used in this study is located in the southern
234 part of Misiones (27°S, 55°W). Native vegetation is a forest dominated by C3 plants. The soil
235 selected is an Acrisol (WRB, 2006). It's a red clay soil, strongly to very strongly acid with a
236 clay content varying from 40% at the surface to 60% at 1m depth. ¹⁴C measurements were
237 made using a new Compact Radiocarbon System called ECHOMICADAS (Environment,
238 Climate, Human, Mini Carbon Dating System) (Tisnérat-Laborde et al., 2015). Details on
239 measurements and sampling can be found in Tifafi et al., *In prep.* Briefly, the soil was
240 sampled in May 2015 at different depths: 0-5cm, 5-10cm, 10-15cm, 15-20cm, 20-30cm, 30-
241 40cm, 40-50cm, 50-60cm, 60-80cm, 80-100cm. All samples were crushed and air-dried. Once

242 in the laboratory, they were homogenized, crushed, randomly subsampled and sieved at
243 200 μm . Then ^{14}C measurements were made using a new Compact Radiocarbon System called
244 *ECHoMICADAS* (Environment, Climate, Human, Mini Carbon Dating System) following the
245 recommendations of Tisnérat-Laborde et al., (2015).

246 For the four sites, the SOC (kg m^{-3}), for each depth z , was calculated using carbon content and
247 bulk density data using the following equation:

$$248 \text{SOC}_z = \text{OCC}_z * \text{BD}_z \quad (8)$$

249 Where *OCC* (wt/wt) is the carbon content and *BD* (kg m^{-3}) is the bulk density.

250 2.4 Different model tests

251 After the implementation of radiocarbon in the model, different tests were carried out (Table
252 2). Here we represent the outputs provided by three simulations:

- 253 i- Simulation using the initial version ORCHIDEE-SOM- ^{14}C (labelled “Control” in
254 figures and tables) in which no changes were made. The diffusion was kept constant
255 throughout the profile ($D = 1.10^{-4} \text{ m}^2 \text{ year}^{-1}$) and the other parameters are those of the
256 detailed version in Camino-Serrano et al., (2017).
- 257 ii- Simulation using the initial version ORCHIDEE-SOM- ^{14}C in which we modified
258 some parameters following He et al. (2016) (“He et al., (2016) parameterization” in
259 figures and tables). In brief, the authors used ^{14}C data from 157 globally distributed
260 soil profiles sampled to 1-meter depth to evaluate CMIP5 models. Their results show
261 that ESMs underestimated the mean age of soil carbon by a factor of more than six and
262 overestimated the carbon sequestration potential of soils by a factor of nearly two. So,
263 the suggestion (that we apply in this simulation) for the IPSL model was to multiply
264 the turnover time of the passive pool by 14 and the flux from slow pool to passive pool
265 by 0.07 (Table 2). The diffusion was kept constant throughout the profile ($D = 1.10^{-4}$
266 $\text{m}^2 \text{ year}^{-1}$) but the turnover time of the passive pool increased from 462 years to 6468
267 years and the flux from the slow pool to the passive pool decreased from 0.07 to
268 0.0049.
- 269 iii- Simulation using the initial version ORCHIDEE-SOM- ^{14}C in which we assume that
270 the diffusion varies as a function of the depth (“Depth-varying diffusion constant” in
271 figures and tables) according to the equation below:

$$272 D(z) = 5.42 \cdot 10^{-4} e^{(-0.04z)} \quad (9)$$

273 Where *D* is the diffusion ($\text{m}^2 \text{ year}^{-1}$) at a specific depth and *z* is the depth. This equation of
274 diffusion varying as a function of depth following Jagercikova et al. (2014) and assumes that
275 bioturbation is higher in the top soil than in deep soil.

276 2.5 Model simulations

277 In order to reach a steady state of the soil module, we ran the model over 12700 years
278 (spinup). The state at the last time step of this spinup was used as the initial state for the
279 simulations. For this, the CRUNCEP meteorological data for the period 1901-1910 were used.
280 This has been applied for Misiones, Feucherolles and Mons. However, for Kissoko, a first
281 spinup similar to the other sites was carried out but a second one (over approximately 4200

282 years) was also done after the end of the first to take into account the change of the land cover
 283 from a tropical forest to a C4 savanna at this site (Schwartz et al., 1992). The atmospheric
 284 CO₂ concentration has been set at 296 ppm (year 1901, (Keeling and Whorf, 2006)) for the
 285 spinups and the F¹⁴C has been set to one corresponding to pre-industrial values. For each site,
 286 specific pH, clay content and bulk density values were used (Table 1). It should be noted that
 287 for these last data, only one value (the mean value on the profile) is provided as input for the
 288 model.

289 The simulations were outputted at a yearly time step, from 1900 to 2011. A yearly
 290 atmospheric CO₂ concentration value (Keeling and Whorf, 2006) is read for the sites. The
 291 same specific pH, clay content and bulk density values were used (Table 1).

292 Figure 2 shows the evolution of the F¹⁴C values in the atmosphere used in our model for
 293 Argentina, Congo and France (Figure 5 from Hua et al. (2013)). The values provided are
 294 classified into five zones, three in the Northern Hemisphere (NH) and two in the Southern
 295 Hemisphere (SH), corresponding to different levels of ¹⁴C. For France, the values correspond
 296 to the NH zone 2, for the Congo to the SH zone 3 and finally for Argentina to the SH zone 1-
 297 2. Thus, for our simulations, a yearly value is read for each site.

298 An F¹⁴C value of 1.8 represents a doubling of the amount of ¹⁴C in atmospheric CO₂. In figure
 299 2, it can be noted that the values recorded in France (northern hemisphere) are higher than
 300 those in the Congo and Argentina (southern hemisphere). This is due to the preponderance of
 301 atmospheric tests in the northern hemisphere and the time required to mix air across the
 302 equator.

303 2.6 Statistical analysis

304 Simulating carbon processes in soil requires comparison between the model outputs and the
 305 measurements to test the model accuracy and possibly implement further improvement.
 306 Statistical analysis based on the statistics of deviation were done to evaluate the model-
 307 measurement discrepancy according to Kobayashi and Salam (2000) (where a detailed
 308 description of the method is provided). Here, we only reproduce the different equations used.
 309 x refers to the model outputs and y to the measurements, while i refers to soil depth. The
 310 intervals of soil depth of the model outputs and the measurements were homogenized by
 311 linearly interpolating the data to common depth intervals defined for each site. The
 312 simulations and data were then compared for each depth interval.

$$313 \quad RMSD = \sqrt{\frac{1}{n} \sum_{i=1}^n (x_i - y_i)^2} \quad (10)$$

314 RMSD is the Root Mean Squared Deviation, which represents the mean distance between
 315 simulation and measurement.

$$316 \quad MSD = \frac{1}{n} \sum_{i=1}^n (x_i - y_i)^2 = (\bar{x} - \bar{y})^2 + \frac{1}{n} \sum_{i=1}^n [(x_i - \bar{x}) - (y_i - \bar{y})]^2 \quad (11)$$

317 MSD, the Mean Squared Deviation, is the square of RMSD. The lower the value of MSD, the
 318 closer the simulation results are to the measurements.

$$319 \quad SB = (\bar{x} - \bar{y})^2 \quad (12)$$

320 Where \bar{x} are the means of x_i (model outputs) and \bar{y}_i (measurements) respectively.

322 SB is a part of the MSD (Eq.14) and represents the bias of the simulation from the
323 measurement.

$$324 \quad SD_s = \sqrt{\frac{1}{n} \sum_{i=1}^n (x_i - \bar{x})^2} \quad (13)$$

325 SD_s is the Standard Deviation of the simulation.

$$326 \quad SD_m = \sqrt{\frac{1}{n} \sum_{i=1}^n (y_i - \bar{y})^2} \quad (14)$$

327 SD_m is the Standard Deviation of the measurements.

$$328 \quad r = \frac{\frac{1}{n} \sum_{i=1}^n (x_i - \bar{x}) - (y_i - \bar{y})}{SD_m SD_s} \quad (15)$$

329 r is the correlation coefficient between the simulation and measurements.

$$330 \quad S D S D = (SD_s - SD_m)^2 \quad (16)$$

331 $S D S D$ is the difference in the magnitude of fluctuation between the simulation and
332 measurements.

$$333 \quad L C S = 2SD_s SD_m(1 - r) \quad (17)$$

334 LCS represents the lack of positive correlation weighted by the standard deviations.

335 The MSD can be therefore be rewritten as:

$$336 \quad MSD = SB + S D S D + L C S \quad (18)$$

337 For the different simulations, the MSD and its components were calculated according to the
338 total soil carbon and to the $F^{14}C$.

339

340 **3 Model results and evaluation**

341 **3.1 Outputs from simulation using the initial version of the model ORCHIDEE-SOM-** 342 **^{14}C (Control)**

343 **3.1.1 Simulated total soil carbon**

344 Results from the initial version of ORCHIDEE-SOM- ^{14}C show that in all the studied sites, the
345 model succeeds in reproducing the trend of the total carbon profiles, with more carbon at the
346 surface which then decreases according to the depth (Figure 3). Moreover, total soil carbon
347 stock simulated down to 2m depth is in accordance with data in the case of Misiones and
348 Feucherolles where the major difference mainly lies on the surface. This results in correlation
349 coefficients of 0.44 and 0.2 respectively (Table 3). For the sites of Kissoko and Mons, an
350 over-estimation of the total soil carbon is found to a depth of 50cm for Kissoko and up to a
351 depth of 120cm for Mons. Correlation coefficients are 0.14 and 0.49 for Kissoko and Mons
352 respectively (Table 3).

353 Metrics presented in Figure 4, showed that this version (ORCHIDEE-SOM- ^{14}C) represents
354 relatively well the observation from Feucherolles ($MSD = 206 \text{ kg C m}^{-6}$), whereas the other
355 are highly overestimated (Kissoko, $MSD = 1343 \text{ kg C m}^{-6}$; Misiones $MSD = 2180 \text{ kg C m}^{-6}$;
356 Mons $MSD = 3355 \text{ kg C m}^{-6}$). By detailing the different components of the MSD (Figure 4),

357 we note that for Mons and Kissoko, standard bias (SB) is the major component of the MSD
358 with contributing 70% and 60% respectively. This reflects that the average of total soil carbon
359 over the soil profile simulated by the model is primarily the origin of the deviation of the
360 model outputs from data. The mean total soil carbon estimated by the model (Table 3) is
361 almost three times higher than the mean total carbon measured for Mons (2.37 kg C m⁻²
362 against 0.8 kg C m⁻² respectively) and it is more than five times that measured for Kissoko
363 (2.44 kg C m⁻² against 0.42 kg C m⁻² respectively). For Mons a net primary production (NPP)
364 of 6.7 t ha⁻¹ yr⁻¹ was estimated by the technical institute for pasture in this region of France
365 based on the annual yields, whereas the model predicts a NPP of 7.5 t ha⁻¹ yr⁻¹. The large
366 overestimation of the SOC stocks may therefore be due to an overestimation of the NPP. This
367 significant gap recorded in the case of the Kissoko site, where the measured SOC is very low,
368 is probably due to an overestimation of decay rates by ORCHIDEE in sandy soils. The
369 correlation coefficient for Mons is relatively high compared to other site (Table 3) whereas
370 Fig. 3 shows that the model performance was not very good for this site. This is mainly due to
371 a large SB whereas other MSD components were rather low.

372

373 However, the main components of MSD for Feucherolles and Misiones are both SB (46% and
374 56% for Feucherolles and Misiones, respectively) and also LCS (53 and 31% for Feucherolles
375 and Misiones, respectively). This means that for these two sites, the deviation between model
376 outputs and measurements is mainly due to a variation of carbon stock estimation throughout
377 the profile. The mean total soil carbon estimated in these both cases (Table 3) is only slightly
378 higher than those measured (2.03 kg C m⁻² estimated against 2.14 kg C m⁻² measured for
379 Misiones and 0.7 kg C m⁻² estimated against 0.68 kg C m⁻² measured for Feucherolles).

380 The vertical profiles of the SOC stock were fairly represented by the model. The
381 overestimation, especially at the top, suggests that the distribution of the litter following the
382 root profile and / or the vertical transport of SOC by diffusion are not correctly described in
383 the model.

384 **3.1.2 Simulated F¹⁴C**

385 Regarding the ¹⁴C activity, bulk F¹⁴C profiles show a classical pattern with higher ¹⁴C activity
386 on the top, slightly influenced by the peak bomb enriched years. Subsequently profiles show
387 decreasing ¹⁴C activity with depth (Figure 5).

388 The estimated profiles (Model-Control) follow the same trend with a decrease from the
389 surface to the depth. However, there is a significant difference between the estimated values
390 and those measured throughout the profile. The statistical analyzes (Figure 6) provide MSD
391 values: 0.02 for Mons and Misiones, 0.03 for Kissoko and 0.09 for Feucherolles. The major
392 component of the MSD in the four sites is the LCS, with a proportion reaching 90% for Mons,
393 80% for Misiones and 70% for Congo, but only 55% for Feucherolles. The high proportions
394 of LCS suggest that the model fails to reproduce the shape of the profile. The lower values
395 estimated by the models reflect a more modern carbon age than in reality. This can be
396 explained, first, by the fact that the root profile puts too much fresh organic carbon in deep

397 soil. Afterwards, in ORCHIDEE, root profile is assumed to follow an exponential function
398 without modulation due to environmental conditions.

399 SB's contribution to the MSD does not exceed 7% for Misiones, Kissoko and Mons but
400 reaches about 40% for Feucherolles. This reflects that the mean value of the $F^{14}C$ estimated
401 by the model and that obtained after the measurements are not very different, except for
402 Feucherolles site (Table 4). Indeed, the average value estimated for Misiones is 0.920, very
403 close to that measured at 0.930, 0.995 for Kissoko against 0.985 measured and 0.860 for
404 Mons against 0.815 measured. Yet, the difference is greater for the Feucherolles site, the
405 estimated value being 0.915 while the measurement is 0.725. This difference might be caused
406 by the low $F^{14}C$ value measured at 150cm (0.257), that the model is not able to capture. This
407 suggests that modeled deep soil carbon is much younger than the observed total soil carbon,
408 probably because ORCHIDEE-SOM simulates a relatively small proportion of passive pool in
409 the lower soil horizons (Figure 7), while an increasing proportion of passive carbon with soil
410 depth could be expected.

411 In brief, SOC stocks are generally overestimated and soil carbon age in deep soils (as shown
412 by the $F^{14}C$) is underestimated, suggesting that the turnover rate of the passive pool is subject
413 to improvements in ORCHIDEE-SOM.

414 **3.2 Outputs from simulation using the initial version of the model ORCHIDEE-SOM- 415 ^{14}C including He's suggestion (He et al., (2016) parameterization)**

416 **3.2.1 Simulated total soil carbon**

417 Figure 3 shows profiles output after He et al (2016)'s suggestion was implemented into
418 ORCHIDEE-SOM- ^{14}C (green dotted curves). Resulting profiles follow the same trend than
419 observations but in this case ("He et al., (2016) parameterization"), the overestimation is very
420 high across the whole profile. This is further confirmed by the metrics analysis (Figure 4).
421 MSD values markedly increased, resulting in an even higher variance. Obviously, the major
422 component of MSD in all cases is the SB (varying from 80% to 87%) reflecting an even more
423 marked overestimation of the mean total carbon estimates: 7.38 kg C m⁻² against 2.14 kg C m⁻²
424 for Misiones, 2.44 kg C m⁻² against 0.42 kg C m⁻² for Kissoko, 2.33 kg C m⁻² against 0.66 kg
425 C m⁻² for Feucherolles and 9.99 kg C m⁻² against 0.8 kg C m⁻² for Mons.

426 **3.2.2 Simulated $F^{14}C$**

427 He et al., (2016) parameterization outputs (Figure 5, green dotted curves) for $F^{14}C$ are once
428 again even further away from observations and MSDs (Figure 6) are much higher, except for
429 Feucherolles. The MSD components for the Feucherolles site show that the LCS increases
430 from 0.05 to 0.06 whereas the SB decreases from 0.04 to 0.03, again reflecting a variation of
431 the profile more than a difference from the means.

432 Improvement of the model-measurement fit for the $F^{14}C$ at 150 cm in Feucherolles confirms
433 that the deep soil carbon simulated by the control version of ORCHIDEE-SOM- ^{14}C was
434 excessively young, since the longer residence time of the passive pool reported by He et al.
435 (2016) resulted in a higher proportion of passive pool across the soil profile (Figure 7), thus
436 improving deep soil carbon age. Nevertheless, this test only improves the simulation of deep

437 soil carbon in Feucherolles. On the contrary, this increase in carbon residence time increases
438 model deviation from observations for all the other cases (Figure 5 and 6).

439 Indeed, taking the priming effect into account in this new version of ORCHIDEE has
440 contributed to a 50% of decrease in carbon storage over the historical period. He et al.,
441 (2016)'s correction was also aimed at reducing this storage and is of the same order of
442 magnitude as the priming effect. Thus, applying He's correction to this version of the model,
443 which takes into account the priming effect, contributes to a double correction for the same
444 target, which then generates this important difference between model outputs and
445 measurements. Moreover, the work of He et al. (2016) is done under the standard
446 parameterization of ORCHIDEE based on Century, while ORCHIDEE-SOM was re-
447 parameterized after adding several different processes, the priming effect among them
448 (Camino-Serrano et al., 2017), which makes it difficult to compare results from between the
449 two studies.

450 **3.3 Outputs from simulation using the initial version of the model ORCHIDEE-SOM- 451 ¹⁴C with diffusion varying according to the depth (Depth-varying diffusion constant)**

452 **3.3.1 Simulated total soil carbon**

453 Fick's law of diffusion is classically used in models to represent bioturbation assuming that
454 soil fauna activity may be represented following the Fick's law of diffusion (Elzein and
455 Balesdent, 1995; Guenet et al., 2013; Koven et al., 2013; O'Brien and Stout, 1978; Wynn et
456 al., 2005). Using a fixed diffusion constant (D in eq. 2) implicitly suggests that soil fauna
457 activity is uniform over the entire soil profile. This is generally the case of several models of
458 diffusion, in particular at the level of an ecosystem (Bruun et al., 2007; Guimberteau et al.,
459 2018; O'Brien and Stout, 1978). However soil faunal activity vary naturally with depth and
460 the diffusion constant should therefore be depth-dependent (Jagercikova et al., 2014).

461 With Depth-varying diffusion constant, the carbon profiles (orange dashed curves) was
462 improved compared to the initial outputs (Control). The overestimation at the surface
463 decreases at the four sites (Figure 3). In particular, the Misiones outputs fit very well the
464 observed profiles. This is confirmed with lower MSDs for the four sites for this version
465 compared to Control (Figure 4).

466 The total SOC stocks simulated according to this third simulation are closer to the measured
467 values and describing the vertical transport of SOC through diffusion varying according to the
468 depth improves significantly the model outputs.

469 **3.3.2 Simulated F¹⁴C**

470 Regarding the F¹⁴C outputs, the simulations using the initial version ORCHIDEE-SOM-¹⁴C in
471 which we assume that the diffusion varies as a function of the depth (Depth-varying diffusion
472 constant) results in an improvement of the F¹⁴C profiles (orange dashes curves), in particular
473 for the sites Misiones, Mons and Kissoko (Figure 5). Statistical analyzes prove it with
474 significantly lower MSDs. In addition, the proportion of LCS is 98%, 92% and 88% for
475 Mons, Misiones and Kissoko, respectively, highlighting an estimated average very close to
476 the measurements with a clear disparity, less marked than with the first two simulations,
477 throughout the profile (Figure 6). Overall, the simulated F¹⁴C to 2 m of depth according to

478 this third simulation are in a better agreement with the measured values, and thus
479 incorporating diffusion that varies with depth significantly improves the model outputs.

480 Using a diffusion coefficient that varies as a function of the depth seems to correct the
481 overestimation of the surface total soil carbon by increasing the proportion of labile soil
482 carbon pools in the first soil layers.

483 When we sum the total soil carbon at each soil layer and look at the relative proportion of
484 each of the soil carbon pools (Figure 7), we note that it is mainly the distribution of the litter
485 according to the depth which varies. In fact, the structural litter proportion is multiplied by
486 about 2 in all four cases, and this proportion remains relatively constant across the profile.
487 This increase in litter proportion has also resulted in a decrease in the passive pool, more
488 pronounced at the surface but also important at depth (except for Feucherolles where the
489 decrease is only marked at the bottom). It suggests that the vertical carbon distribution, which
490 is largely modified by the diffusion coefficient, greatly impacts the SOC and ^{14}C profiles,
491 which is in line with Dwivedi et al. (2017) who found that the vertical carbon input profiles
492 were important controls over the ^{14}C depth distribution.

493 In this study, the vertical transport of SOC and litter through diffusion has been improved by
494 varying diffusion according to the depth. Further model development should explore the
495 impact of the other processes defining the soil carbon pools vertical distribution and
496 especially the distribution of the litter according to the root profile.

497 Overall, by using radiocarbon (^{14}C) measurements we have been able to diagnose internal
498 model biases (underestimation of deep soil carbon age) and to propose further model
499 improvements (depth-dependent diffusion). Therefore, the use of radiocarbon (^{14}C) tracers in
500 global models emerges as a promising tool to constrain not only SOC turnover times in the
501 long-term (He et al., 2016), but also internal SOC processes and fluxes that have no direct
502 comparison with field measurements. Nevertheless, the model evaluation performed here on
503 only four sites should be considered as proof of concept and more in depth evaluation are
504 needed, in particular using a large ^{14}C database available at global scale (Balesdent et al.,
505 2018; Mathieu et al., 2015). Indeed, the $F^{14}\text{C}$ is largely controlled by pedo-climatic conditions
506 such as clay content, climate and mineralogy (Mathieu et al., 2015) and the range of situations
507 we covered here is relatively limited.

508

509 **4 conclusion**

510 ORCHIDEE-SOM- ^{14}C , is one of the first land surface models that incorporates the ^{14}C
511 dynamics in the soil (Koven et al., 2013). Its starting point is ORCHIDEE-SOM, a recently
512 developed soil model. We evaluated the new model ORCHIDEE-SOM- ^{14}C for four sites in
513 different biomes. The model almost managed to reproduce the soil organic carbon stocks and
514 the ^{14}C content along the vertical profiles at all four sites. However, an overestimation of the
515 total carbon stock throughout the profile was noted, with the greatest deviation at the surface.
516 By using radiocarbon (^{14}C) measurements, we have been able to diagnose internal model
517 biases (underestimation of deep soil carbon age) and to propose further model improvements
518 (depth-dependent diffusion). These results demonstrate the importance of depth-dependent

519 diffusion to improving model outputs with regards to observations. This suggests that, from
520 now on, model improvements should mainly focus on a depth dependent parameterization.
521 We limited our work here to depth-varying diffusion, but other parameters are also depth
522 dependent and should be represented as such in the next version of the model. For instance,
523 belowground litter production in the model is simply represented by an exponential law
524 without any representation of the effect of resource distribution on root profile (e.g. water or
525 nutrients). This is a complex task in a land surface model running at large scale with a
526 classical resolution of 0.5°, but the soil modules of land surface models are quite sensitive to
527 the NPP (Camino-Serrano et al., 2018; Todd-Brown et al., 2013) and a better constraint on the
528 profile of the below ground litter production would likely improve the model performance.
529 Furthermore, here we used only one averaged value over the soil profile for soil boundary
530 conditions (texture, pH, bulk density) but those variables are known to impact the F¹⁴C
531 (Mathieu et al., 2015) and change with depth (Barré et al., 2009) and depth-varying boundary
532 conditions may also help to improve the model. Finally, the next step will deal with the
533 comparison of model outputs to data at larger scales to be able to run the new version
534 ORCHIDEE-SOM-¹⁴C at both regional and global scales.

535

536

537

538

539 **Code availability**

540 The version of the code is freely available here:

541 http://forge.ipsl.jussieu.fr/orchidee/wiki/GroupActivities/CodeAvailabilityPublication/ORCHIDEE_gmd-2018-14C

543

544 **Acknowledgement**

545 This study, part of the MT's PhD, financed by the University of Versailles Saint Quentin, is
546 within the scope of the ANR-14-CE01-0004 DeDyCAS project. Marta Camino-Serrano
547 acknowledges funding from the European Research Council Synergy grant ERC- 2013-SyG-
548 610028 IMBALANCE-P. Part of the data were acquired in the frame of the AGRIPED
549 project (ANR 2010 BLAN 605). We thank Matthew McGrath for his valuable comments on
550 the manuscript.

551

552 **References**

- 553 Ahrens, B., Braakhekke, M. C., Guggenberger, G., Schrumpf, M. and Reichstein, M.:
554 Contribution of sorption, DOC transport and microbial interactions to the 14C age of a soil
555 organic carbon profile: Insights from a calibrated process model, *Soil Biol. Biochem.*, 88,
556 390–402, doi:10.1016/j.soilbio.2015.06.008, 2015.
- 557 Balesdent, J. and Guillet, B.: Les datations par le 14C des matières organiques des sols.

558 Contribution à l'étude de l'humification et du renouvellement des substances
559 humiqueétriques, *Sci. du sol*, 2, 93–111, 1982.

560 Balesdent, J., Basile-Doelsch, I., Chadoeuf, J., Cornu, S., Derrien, D., Fekiacova, Z. and
561 Hatté, C.: Atmosphere–soil carbon transfer as a function of soil depth, *Nature*, 23, 1,
562 doi:10.1038/s41586-018-0328-3, 2018.

563 Barré, P., Berger, G. and Velde, B.: How element translocation by plants may stabilize illitic
564 clays in the surface of temperate soils, *Geoderma*, 151(1–2), 22–30,
565 doi:10.1016/j.geoderma.2009.03.004, 2009.

566 Braakhekke, M., Beer, C., Schrumpf, M., Ekici, A., Ahrens, B., Hoosbeek, M. R., Kruijt, B.,
567 Kabat, P. and Reichstein, M.: The use of radiocarbon to constrain current and future soil
568 organic matter turnover and transport in a temperate forest, *J. Geophys. Res. Biogeosciences*,
569 372–391, doi:10.1002/2013JG002420.Received, 2014.

570 Braakhekke, M. C., Beer, C., Hoosbeek, M. R., Reichstein, M., Kruijt, B., Schrumpf, M. and
571 Kabat, P.: SOMPROF: A vertically explicit soil organic matter model, *Ecol. Modell.*,
572 222(10), 1712–1730, doi:10.1016/j.ecolmodel.2011.02.015, 2011.

573 Bruun, S., Christensen, B. T., Thomsen, I. K., Jensen, E. S. and Jensen, L. S.: Modeling
574 vertical movement of organic matter in a soil incubated for 41 years with ¹⁴C labeled straw,
575 *Soil Biol. Biochem.*, 39(1), 368–371, doi:10.1016/j.soilbio.2006.07.003, 2007.

576 Camino-Serrano, M., Guenet, B., Luyssaert, S., Ciais, P., Bastrikov, V., De Vos, B., Gielen,
577 B., Gleixner, G., Jornet-Puig, A., Kaiser, K., Kothawala, D., Lauerwald, R., Peñuelas, J.,
578 Schrumpf, M., Vicca, S., Vuichard, N., Walmsley, D. and Janssens, I. A.: ORCHIDEE-SOM:
579 Modeling soil organic carbon (SOC) and dissolved organic carbon (DOC) dynamics along
580 vertical soil profiles in Europe, *Geosci. Model Dev.*, 11, 937–957, doi:10.5194/gmd-11-937-
581 2018, 2018.

582 Coleman, K., Jenkinson, D. S., Crocker, G. J., Grace, P. R., Klír, J., Körschens, M., Poulton,
583 P. R. and Richter, D. D.: Simulating trends in soil organic carbon in long-term experiments
584 using RothC-26.3, *Geoderma*, 81(1–2), 29–44, doi:10.1016/S0016-7061(97)00079-7, 1997.

585 Cottreau, E., Arnold, M., Moreau, C., Baqué, D., Bavay, D., Caffy, I., Comby, C.,
586 Dumoulin, J.-P., Hain, S., Perron, M., Salomon, J. and Setti, V.: Artemis, the New ¹⁴C AMS
587 at LMC14 in Saclay, France, *Radiocarbon*, 49(2), 291–299, doi:10.2458/azu_js_rc.49.2928,
588 2007.

589 Delibrias, G., Guillier, M. T. and Labeyrie, J.: Saclay natural radiocarbon measurements i,
590 *Radiocarbon*, 6, 233–250, 1964.

591 Ducoudré, N. I., Laval, K. and Perrier, A.: SECHIBA, a New Set of Parameterizations of the
592 Hydrologic Exchanges at the Land-Atmosphere Interface within the LMD Atmospheric
593 General Circulation Model, *J. Clim.*, 6(2), 248–273, doi:10.1175/1520-
594 0442(1993)006<0248:SANSOP>2.0.CO;2, 1993.

595 Dwivedi, D., Riley, W., Torn, M., Spycher, N., Maggi, F. and Tang, J.: Mineral properties,
596 microbes, transport, and plant-input profiles control vertical distribution and age of soil
597 carbon stocks, *Soil Biol. Biochem.*, 107(2017), 244–259, doi:10.1016/j.soilbio.2016.12.019,
598 2017.

599 Elliott, E. T., Paustian, K. and Frey, S. D.: Modeling the Measurable or Measuring the
600 Modelable: A Hierarchical Approach to Isolating Meaningful Soil Organic Matter
601 Fractionations, in *Evaluation of Soil Organic Matter Models: Using Existing Long-Term*
602 *Datasets*, vol. 1994, pp. 161–179., 1996.

603 Elzein, A. and Balesdent, J.: Mechanistic Simulation of vertical distribution of carbon
604 concentrations and residence times in soils, *Soil Sci. Soc. Am. J.*, 59, 1328–1335,
605 doi:10.1017/CBO9781107415324.004, 1995.

606 Epron, D., Marsden, C., M'Bou, A. T., Saint-André, L., d'Annunzio, R. and Nouvellon, Y.:
607 Soil carbon dynamics following afforestation of a tropical savannah with Eucalyptus in
608 Congo, *Plant Soil*, 323(1), 309–322, doi:10.1007/s11104-009-9939-7, 2009.

609 Godwin, H.: Half-life of radiocarbon, *Nature*, 195(4845), 984, doi:10.1038/195984a0, 1962.

610 Guenet, B., Eglin, T., Vasilyeva, N., Peylin, P., Ciais, P. and Chenu, C.: The relative
611 importance of decomposition and transport mechanisms in accounting for soil organic carbon
612 profiles, *Biogeosciences*, 10(4), 2379–2392, doi:10.5194/bg-10-2379-2013, 2013.

613 Guenet, B., Moyano, F. E., Peylin, P., Ciais, P. and Janssens, I. A.: Towards a representation
614 of priming on soil carbon decomposition in the global land biosphere model ORCHIDEE
615 (version 1.9.5.2), *Geosci. Model Dev.*, 9(2), 841–855, doi:10.5194/gmd-9-841-2016, 2016.

616 Guimberteau, M., Zhu, D., Maignan, F., Huang, Y., Yue, C., Dantec-Nédélec, S., Ottlé, C.,
617 Jornet-Puig, A., Bastos, A., Laurent, P., Goll, D., Bowring, S., Chang, J., Guenet, B., Tifafi,
618 M., Peng, S., Krinner, G., Ducharne, A., Wang, F., Wang, T., Wang, X., Wang, Y., Yin, Z.,
619 Lauerwald, R., Joetzjer, E., Qiu, C., Kim, H. and Ciais, P.: ORCHIDEE-MICT (revision
620 4126), a land surface model for the high-latitudes: model description and validation, *Geosci.
621 Model Dev.*, 11, 121–163, doi:10.5194/gmd-2017-122, 2018.

622 He, Y., Trumbore, S. E., Torn, M. S., Harden, J. W., Vaughn, L. J. S., Allison, S. D. and
623 Randerson, J. T.: Radiocarbon constraints imply reduced carbon uptake by soils during the
624 21st century, *Science* (80-.), 353(6306), 1419–1424, 2016.

625 Hua, Q., Barbetti, M. and Rakowski, A. Z.: Atmospheric Radiocarbon for the Period 1950–
626 2010, *Radiocarbon*, 55(4), 2059–2072, doi:10.2458/azu_js_rc.v55i2.16177, 2013.

627 Jagercikova, M., Evrard, O., Balesdent, J., Lefèvre, I. and Cornu, S.: Modeling the migration
628 of fallout radionuclides to quantify the contemporary transfer of fine particles in Luvisol
629 profiles under different land uses and farming practices, *Soil Tillage Res.*, 140(2014), 82–97,
630 doi:10.1016/j.still.2014.02.013, 2014.

631 Jagercikova, M., Cornu, S., Boulès, D., Evrard, O., Hatté, C. and Balesdent, J.:
632 Quantification of vertical solid matter transfers in soils during pedogenesis by a multi-tracer
633 approach, *J. Soils Sediments*, 17(2), 408–422, doi:10.1007/s11368-016-1560-9, 2017.

634 Jastrow, J. D., Amonette, J. E. and Bailey, V. L.: Mechanisms controlling soil carbon turnover
635 and their potential application for enhancing carbon sequestration, *Clim. Change*, 80, 5–23,
636 doi:10.1007/s10584-006-9178-3, 2007.

637 Kalnay, E., Kanamitsu, M., Kistler, R., Collins, W., Deaven, D., Gandin, L., Iredell, M., Saha,
638 S., White, G., Woollen, J., Zhu, Y., Chelliah, M., Ebisuzaki, W., Higgins, W., Janowiak, J.,
639 Mo, K. C., Ropelewski, C., Wang, J., Leetmaa, a., Reynolds, R., Jenne, R. and Joseph, D.:
640 The NCEP/NCAR 40-year reanalysis project, *Bull. Am. Meteorol. Soc.*, 77(3), 437–471,
641 doi:10.1175/1520-0477(1996)077<0437:TNYRP>2.0.CO;2, 1996.

642 Keeling, C. D. and Whorf, T. P.: Atmospheric CO₂ records from sites in the SIO air sampling
643 network, Oak Ridge Natl. Lab. U.S. Dept. of Energy, Oak Ridge, Tenn., 2006.

644 Keyvanshokouhi, S., Cornu, S., Samouëlian, A. and Finke, P.: Evaluating SoilGen2 as a tool
645 for projecting soil evolution induced by global change, *Sci. Total Environ.*, 571, 110–123,
646 doi:10.1016/j.scitotenv.2016.07.119, 2016.

647 Kobayashi, K. and Salam, M. .: Comparing simulated and measured values using mean
648 squared deviation and its components, *Agron. J.*, 92(2), 345–352 [online] Available from:
649 [http://scholar.google.com/scholar?hl=en&btnG=Search&q=intitle:Comparing+Simulated+and](http://scholar.google.com/scholar?hl=en&btnG=Search&q=intitle:Comparing+Simulated+and+Measured+Values+Using+Mean+Squared+Deviation+and+its+Components#0)
650 [+Measured+Values+Using+Mean+Squared+Deviation+and+its+Components#0](http://scholar.google.com/scholar?hl=en&btnG=Search&q=intitle:Comparing+Simulated+and+Measured+Values+Using+Mean+Squared+Deviation+and+its+Components#0) (Accessed 2
651 February 2012), 2000.

652 Koven, C. D., Riley, W. J., Subin, Z. M., Tang, J. Y., Torn, M. S., Collins, W. D., Bonan, G.
653 B., Lawrence, D. M. and Swenson, S. C.: The effect of vertically resolved soil
654 biogeochemistry and alternate soil C and N models on C dynamics of CLM4, *Biogeosciences*,
655 10(11), 7109–7131, doi:10.5194/bg-10-7109-2013, 2013.

656 Krinner, G., Viovy, N., de Noblet-Ducoudré, N., Ogée, J., Polcher, J., Friedlingstein, P.,
657 Ciais, P., Sitch, S. and Prentice, I. C.: A dynamic global vegetation model for studies of the
658 coupled atmosphere-biosphere system, *Glob. Biogeochem. Cycles*, 19(1),
659 doi:10.1029/2003GB002199, 2005.

660 Laclau, J. P., Bouillet, J. P. and Ranger, J.: Dynamics of biomass and nutrient accumulation in
661 a clonal plantation of Eucalyptus in Congo, *For. Ecol. Manage.*, 128(3), 181–196,
662 doi:10.1016/S0378-1127(99)00146-2, 2000.

663 Mathieu, J. a., Hatté, C., Balesdent, J. and Parent, É.: Deep soil carbon dynamics are driven
664 more by soil type than by climate: a worldwide meta-analysis of radiocarbon profiles, *Glob.*
665 *Chang. Biol.*, n/a-n/a, doi:10.1111/gcb.13012, 2015.

666 Mitchell, T. D., Carter, T. R., Jones, P. D., Hulme, M. and New, M.: A comprehensive set of
667 high-resolution grids of monthly climate for Europe and the globe: the observed record
668 (1901–2000) and 16 scenarios (2001–2100), ... *Cent. Clim. ...*, (July), 1–30 [online]
669 Available from: <http://www.tyndall.ac.uk/sites/default/files/wp55.pdf>, 2004.

670 Morrás, H., Moretti, L., Piccolo, G. and Zech, W.: Genesis of subtropical soils with stony
671 horizons in NE Argentina: Autochthony and polygenesis, *Quat. Int.*, 196(1), 137–159,
672 doi:10.1016/j.quaint.2008.07.001, 2009.

673 O'Brien, B. J. and Stout, J. D.: Movement and turnover of soil organic matter as indicated by
674 carbon isotope measurements, *Soil Biol. Biochem.*, 10(4), 309–317, doi:10.1016/0038-
675 0717(78)90028-7, 1978.

676 Parton, W., Schimel, D. S., Cole, C. and Ojima, D.: Analysis of factors controlling soil
677 organic matter levels in Great Plains grasslands, *Soil Sci. Soc. Am. J.*, 51, 1173–1179 [online]
678 Available from: [http://agris.fao.org/agris-](http://agris.fao.org/agris-search/search/display.do?f=1990/US/US90315.xml;US9004388)
679 [search/search/display.do?f=1990/US/US90315.xml;US9004388](http://agris.fao.org/agris-search/search/display.do?f=1990/US/US90315.xml;US9004388) (Accessed 27 July 2011),
680 1987.

681 Parton, W. J., Stewart, J. W. B. and Cole, C. V.: Dynamics of C, N, P and S in grassland soils:
682 a model, *Biogeochemistry*, 5(1), 109–131, doi:10.1007/BF02180320, 1988.

683 Reimer, P. J., Brown, T. A. and Reimer, R. W.: Discussion: reporting and calibration of post-
684 bomb 14C data., *Radiocarbon*, 46(1), 1299–1304, doi:10.2458/azu_js_rc.46.4183, 2004.

685 Rosnay, P. de and Polcher, J.: MOdelling root water uptake in a complex land surface scheme
686 coupled to a GCM, *Hydrol. Earth Syst. ...*, 2, 239–255 [online] Available from:
687 <http://adsabs.harvard.edu/abs/1998HESS....2..239D> (Accessed 26 March 2013), 1998.

688 Scharpenseel, H. W. and Schiffmann, H.: Radiocarbon dating of soils, a review, *Zeitschrift*
689 *für Pflanzenernährung und Bodenkd.*, 140(2), 159–174, doi:10.1002/jpln.19771400205, 1977.

690 Schwartz, D., Mariotti, A., Trouve, C., Van Den Borg, K. and Guillet, B.: Etude des profils
691 isotopiques 13C et 14C d'un sol ferrallitique sableux du littoral congolais : implications sur la

692 dynamique de la matière organique et l'histoire de la végétation, *Comptes Rendus l'Académie*
693 *des Sci. 2 Mécanique...*, 1992, 315, p. 1411-1417. ISSN 0249-6305, 315, 1411-1417, 1992.

694 Sitch, S., Smith, B., Prentice, I. C., Arneth, a., Bondeau, a., Cramer, W., Kaplan, J. O.,
695 Levis, S., Lucht, W., Sykes, M. T., Thonicke, K. and Venevsky, S.: Evaluation of ecosystem
696 dynamics, plant geography and terrestrial carbon cycling in the LPJ dynamic global
697 vegetation model, *Glob. Chang. Biol.*, 9(2), 161-185, doi:10.1046/j.1365-2486.2003.00569.x,
698 2003.

699 Stuiver, M. and Polach, H. A.: Reporting of ¹⁴C data, *Radiocarbon*, 19(3), 355-363,
700 doi:10.1016/j.forsciint.2010.11.013, 1977.

701 Taylor, K. E., Stouffer, R. J. and Meehl, G. a.: An overview of CMIP5 and the experiment
702 design, *Bull. Am. Meteorol. Soc.*, 93(4), 485-498, doi:10.1175/BAMS-D-11-00094.1, 2012.

703 Tisnérat-Laborde, N., Thil, F., Synal, H.-A., Hatté, C., Cersoy, S., Gauthier, C., Kaltnecker,
704 E., Massault, M., Michelot, J.-L., Noret, A., Noury, C., Siani, G., Tombret, O., Vigne, J.-D.,
705 Wacker, L. and Zazzo, A.: A new compact AMS facility measuring ¹⁴C dedicated to
706 Environment, Climate and Human Sciences, in 22nd International Radiocarbon Conference,
707 Dakar, Senegal. November 2015. Oral presentation, pp. 16-20., 2015.

708 Todd-Brown, K. E. O., Randerson, J. T., Post, W. M., Hoffman, F. M., Tarnocai, C., Schuur,
709 E. a. G. and Allison, S. D.: Causes of variation in soil carbon simulations from CMIP5 Earth
710 system models and comparison with observations, *Biogeosciences*, 10(3), 1717-1736,
711 doi:10.5194/bg-10-1717-2013, 2013.

712 Trumbore, S.: Age of Soil Organic Matter and Soil Respiration : Radiocarbon Constraints on
713 Belowground C Dynamics, *Ecol. Appl.*, 10(2), 399-411, doi:10.1890/1051-
714 0761(2000)010[0399:AOSOMA]2.0.CO;2, 2000.

715 Wieder, W. R., Bonan, G. B. and Allison, S. D.: Global soil carbon projections are improved
716 by modelling microbial processes, *Nat. Clim. Chang.*, 3(8), 1-4, doi:10.1038/nclimate1951,
717 2013.

718 WRB: World reference base for soil resources 2006: a framework for international
719 classification, correlation and communication., 2006.

720 Wynn, J. G., Bird, M. I. and Wong, V. N. L.: Rayleigh distillation and the depth profile of
721 ¹³C/¹²C ratios of soil organic carbon from soils of disparate texture in Iron Range National
722 Park, Far North Queensland, Australia, *Geochim. Cosmochim. Acta*, 69(8), 1961-1973, 2005.

723

724 Balesdent, J. and Guillet, B.: Les datations par le ¹⁴C des matières organiques des sols.
725 Contribution à l'étude de l'humification et du renouvellement des substances
726 humiqueétriques, *Sci. du sol*, 2, 93-111, 1982.

727 Balesdent, J., Basile-Doelsch, I., Chadoeuf, J., Cornu, S., Derrien, D., Fekiacova, Z. and
728 Hatté, C.: Atmosphere-soil carbon transfer as a function of soil depth, *Nature*, 23, 1,
729 doi:10.1038/s41586-018-0328-3, 2018.

730 Barré, P., Berger, G. and Velde, B.: How element translocation by plants may stabilize illitic
731 clays in the surface of temperate soils, *Geoderma*, 151(1-2), 22-30,
732 doi:10.1016/j.geoderma.2009.03.004, 2009.

733 Braakhekke, M., Beer, C., Schrumpf, M., Ekici, A., Ahrens, B., Hoosbeek, M. R., Kruijt, B.,
734 Kabat, P. and Reichstein, M.: The use of radiocarbon to constrain current and future soil
735 organic matter turnover and transport in a temperate forest, *J. Geophys. Res. Biogeosciences*,

736 372–391, doi:10.1002/2013JG002420.Received, 2014.

737 Braakhekke, M. C., Beer, C., Hoosbeek, M. R., Reichstein, M., Kruijt, B., Schrumpf, M. and
738 Kabat, P.: SOMPROF: A vertically explicit soil organic matter model, *Ecol. Modell.*,
739 222(10), 1712–1730, doi:10.1016/j.ecolmodel.2011.02.015, 2011.

740 Bruun, S., Christensen, B. T., Thomsen, I. K., Jensen, E. S. and Jensen, L. S.: Modeling
741 vertical movement of organic matter in a soil incubated for 41 years with ¹⁴C labeled straw,
742 *Soil Biol. Biochem.*, 39(1), 368–371, doi:10.1016/j.soilbio.2006.07.003, 2007.

743 Camino-Serrano, M., Guenet, B., Luyssaert, S., Ciais, P., Bastrikov, V., De Vos, B., Gielen,
744 B., Gleixner, G., Jornet-Puig, A., Kaiser, K., Kothawala, D., Lauerwald, R., Peñuelas, J.,
745 Schrumpf, M., Vicca, S., Vuichard, N., Walmsley, D. and Janssens, I. A.: ORCHIDEE-SOM:
746 Modeling soil organic carbon (SOC) and dissolved organic carbon (DOC) dynamics along
747 vertical soil profiles in Europe, *Geosci. Model Dev.*, 11, 937–957, doi:10.5194/gmd-11-937-
748 2018, 2018.

749 Coleman, K., Jenkinson, D. S., Crocker, G. J., Grace, P. R., Klír, J., Körschens, M., Poulton,
750 P. R. and Richter, D. D.: Simulating trends in soil organic carbon in long-term experiments
751 using RothC-26.3, *Geoderma*, 81(1–2), 29–44, doi:10.1016/S0016-7061(97)00079-7, 1997.

752 Cottreau, E., Arnold, M., Moreau, C., Baqué, D., Bavay, D., Caffy, I., Comby, C.,
753 Dumoulin, J.-P., Hain, S., Perron, M., Salomon, J. and Setti, V.: Artemis, the New ¹⁴C AMS
754 at LMC14 in Saclay, France, *Radiocarbon*, 49(2), 291–299, doi:10.2458/azu_js_rc.49.2928,
755 2007.

756 Delibrias, G., Guillier, M. T. and Labeyrie, J.: Saclay natural radiocarbon measurements i,
757 *Radiocarbon*, 6, 233–250, 1964.

758 Ducoudré, N. I., Laval, K. and Perrier, A.: SECHIBA, a New Set of Parameterizations of the
759 Hydrologic Exchanges at the Land-Atmosphere Interface within the LMD Atmospheric
760 General Circulation Model, *J. Clim.*, 6(2), 248–273, doi:10.1175/1520-
761 0442(1993)006<0248:SANSOP>2.0.CO;2, 1993.

762 Dwivedi, D., Riley, W., Torn, M., Spycher, N., Maggi, F. and Tang, J.: Mineral properties,
763 microbes, transport, and plant-input profiles control vertical distribution and age of soil
764 carbon stocks, *Soil Biol. Biochem.*, 107(2017), 244–259, doi:10.1016/j.soilbio.2016.12.019,
765 2017.

766 Elliott, E. T., Paustian, K. and Frey, S. D.: Modeling the Measurable or Measuring the
767 Modelable: A Hierarchical Approach to Isolating Meaningful Soil Organic Matter
768 Fractionations, in *Evaluation of Soil Organic Matter Models: Using Existing Long-Term
769 Datasets*, vol. 1994, pp. 161–179., 1996.

770 Elzein, A. and Balesdent, J.: Mechanistic Simulation of vertical distribution of carbon
771 concentrations and residence times in soils, *Soil Sci. Soc. Am. J.*, 59, 1328–1335,
772 doi:10.1017/CBO9781107415324.004, 1995.

773 Epron, D., Marsden, C., M'Bou, A. T., Saint-André, L., d'Annunzio, R. and Nouvellon, Y.:
774 Soil carbon dynamics following afforestation of a tropical savannah with Eucalyptus in
775 Congo, *Plant Soil*, 323(1), 309–322, doi:10.1007/s11104-009-9939-7, 2009.

776 Godwin, H.: Half-life of radiocarbon, *Nature*, 195(4845), 984, doi:10.1038/195984a0, 1962.

777 Guenet, B., Eglin, T., Vasilyeva, N., Peylin, P., Ciais, P. and Chenu, C.: The relative
778 importance of decomposition and transport mechanisms in accounting for soil organic carbon
779 profiles, *Biogeosciences*, 10(4), 2379–2392, doi:10.5194/bg-10-2379-2013, 2013.

780 Guenet, B., Moyano, F. E., Peylin, P., Ciais, P. and Janssens, I. A.: Towards a representation
781 of priming on soil carbon decomposition in the global land biosphere model ORCHIDEE
782 (version 1.9.5.2), *Geosci. Model Dev.*, 9(2), 841–855, doi:10.5194/gmd-9-841-2016, 2016.

783 Guimberteau, M., Zhu, D., Maignan, F., Huang, Y., Yue, C., Dantec-Nédélec, S., Ottlé, C.,
784 Jornet-Puig, A., Bastos, A., Laurent, P., Goll, D., Bowring, S., Chang, J., Guenet, B., Tifafi,
785 M., Peng, S., Krinner, G., Ducharne, A., Wang, F., Wang, T., Wang, X., Wang, Y., Yin, Z.,
786 Lauerwald, R., Joetzjer, E., Qiu, C., Kim, H. and Ciais, P.: ORCHIDEE-MICT (revision
787 4126), a land surface model for the high-latitudes: model description and validation, *Geosci.
788 Model Dev. Discuss.*, 1–65, doi:10.5194/gmd-2017-122, 2017.

789 He, Y., Trumbore, S. E., Torn, M. S., Harden, J. W., Vaughn, L. J. S., Allison, S. D. and
790 Randerson, J. T.: Radiocarbon constraints imply reduced carbon uptake by soils during the
791 21st century, *Science* (80-.), 353(6306), 1419–1424, 2016.

792 Hua, Q., Barbetti, M. and Rakowski, A. Z.: Atmospheric Radiocarbon for the Period 1950–
793 2010, *Radiocarbon*, 55(4), 2059–2072, doi:10.2458/azu_js_rc.v55i2.16177, 2013.

794 Jagercikova, M., Evrard, O., Balesdent, J., Lefèvre, I. and Cornu, S.: Modeling the migration
795 of fallout radionuclides to quantify the contemporary transfer of fine particles in Luvisol
796 profiles under different land uses and farming practices, *Soil Tillage Res.*, 140(2014), 82–97,
797 doi:10.1016/j.still.2014.02.013, 2014.

798 Jagercikova, M., Cornu, S., Boulrès, D., Evrard, O., Hatté, C. and Balesdent, J.:
799 Quantification of vertical solid matter transfers in soils during pedogenesis by a multi-tracer
800 approach, *J. Soils Sediments*, 17(2), 408–422, doi:10.1007/s11368-016-1560-9, 2017.

801 Jastrow, J. D., Amonette, J. E. and Bailey, V. L.: Mechanisms controlling soil carbon turnover
802 and their potential application for enhancing carbon sequestration, *Clim. Change*, 80, 5–23,
803 doi:10.1007/s10584-006-9178-3, 2007.

804 Kalnay, E., Kanamitsu, M., Kistler, R., Collins, W., Deaven, D., Gandin, L., Iredell, M., Saha,
805 S., White, G., Woollen, J., Zhu, Y., Chelliah, M., Ebisuzaki, W., Higgins, W., Janowiak, J.,
806 Mo, K. C., Ropelewski, C., Wang, J., Leetmaa, a., Reynolds, R., Jenne, R. and Joseph, D.:
807 The NCEP/NCAR 40-year reanalysis project, *Bull. Am. Meteorol. Soc.*, 77(3), 437–471,
808 doi:10.1175/1520-0477(1996)077<0437:TNYRP>2.0.CO;2, 1996.

809 Keeling, C. D. and Whorf, T. P.: Atmospheric CO₂ records from sites in the SIO air sampling
810 network, Oak Ridge Natl. Lab. U.S. Dept. of Energy, Oak Ridge, Tenn., 2006.

811 Keyvanshokouhi, S., Cornu, S., Samouëlian, A. and Finke, P.: Evaluating SoilGen2 as a tool
812 for projecting soil evolution induced by global change, *Sci. Total Environ.*, 571, 110–123,
813 doi:10.1016/j.scitotenv.2016.07.119, 2016.

814 Kobayashi, K. and Salam, M. : Comparing simulated and measured values using mean
815 squared deviation and its components, *Agron. J.*, 92(2), 345–352 [online] Available from:
816 <http://scholar.google.com/scholar?hl=en&btnG=Search&q=intitle:Comparing+Simulated+and+Measured+Values+Using+Mean+Squared+Deviation+and+its+Components#0> (Accessed 2
817 February 2012), 2000.

819 Koven, C. D., Riley, W. J., Subin, Z. M., Tang, J. Y., Torn, M. S., Collins, W. D., Bonan, G.
820 B., Lawrence, D. M. and Swenson, S. C.: The effect of vertically resolved soil
821 biogeochemistry and alternate soil C and N models on C dynamics of CLM4, *Biogeosciences*,
822 10(11), 7109–7131, doi:10.5194/bg-10-7109-2013, 2013.

823 Krinner, G., Viovy, N., de Noblet-Ducoudré, N., Ogée, J., Polcher, J., Friedlingstein, P.,
824 Ciais, P., Sitch, S. and Prentice, I. C.: A dynamic global vegetation model for studies of the

825 coupled atmosphere-biosphere system, *Glob. Biogeochem. Cycles*, 19(1),
826 doi:10.1029/2003GB002199, 2005.

827 Laclau, J. P., Bouillet, J. P. and Ranger, J.: Dynamics of biomass and nutrient accumulation in
828 a clonal plantation of Eucalyptus in Congo, *For. Ecol. Manage.*, 128(3), 181–196,
829 doi:10.1016/S0378-1127(99)00146-2, 2000.

830 Mathieu, J. a., Hatté, C., Balesdent, J. and Parent, É.: Deep soil carbon dynamics are driven
831 more by soil type than by climate: a worldwide meta-analysis of radiocarbon profiles, *Glob.*
832 *Chang. Biol.*, n/a-n/a, doi:10.1111/gcb.13012, 2015.

833 Mitchell, T. D., Carter, T. R., Jones, P. D., Hulme, M. and New, M.: A comprehensive set of
834 high-resolution grids of monthly climate for Europe and the globe: the observed record
835 (1901–2000) and 16 scenarios (2001–2100), ... *Cent. Clim. ...*, (July), 1–30 [online]
836 Available from: <http://www.tyndall.ac.uk/sites/default/files/wp55.pdf>, 2004.

837 Morrás, H., Moretti, L., Piccolo, G. and Zech, W.: Genesis of subtropical soils with stony
838 horizons in NE Argentina: Autochthony and polygenesis, *Quat. Int.*, 196(1), 137–159,
839 doi:10.1016/j.quaint.2008.07.001, 2009.

840 O'Brien, B. J. and Stout, J. D.: Movement and turnover of soil organic matter as indicated by
841 carbon isotope measurements, *Soil Biol. Biochem.*, 10(4), 309–317, doi:10.1016/0038-
842 0717(78)90028-7, 1978.

843 Parton, W., Schimel, D. S., Cole, C. and Ojima, D.: Analysis of factors controlling soil
844 organic matter levels in Great Plains grasslands, *Soil Sci. Soc. Am. J.*, 51, 1173–1179 [online]
845 Available from: [http://agris.fao.org/agris-
846 search/search/display.do?f=1990/US/US90315.xml;US9004388](http://agris.fao.org/agris-search/search/display.do?f=1990/US/US90315.xml;US9004388) (Accessed 27 July 2011),
847 1987.

848 Parton, W. J., Stewart, J. W. B. and Cole, C. V.: Dynamics of C, N, P and S in grassland soils:
849 a model, *Biogeochemistry*, 5(1), 109–131, doi:10.1007/BF02180320, 1988.

850 Reimer, P. J., Brown, T. A. and Reimer, R. W.: Discussion: reporting and calibration of post-
851 bomb 14C data., *Radiocarbon*, 46(1), 1299–1304, doi:10.2458/azu_js_rc.46.4183, 2004.

852 Rosnay, P. de and Polcher, J.: MOdelling root water uptake in a complex land surface scheme
853 coupled to a GCM, *Hydrol. Earth Syst. ...*, 2, 239–255 [online] Available from:
854 <http://adsabs.harvard.edu/abs/1998HESS....2..239D> (Accessed 26 March 2013), 1998.

855 Scharpenseel, H. W. and Schiffmann, H.: Radiocarbon dating of soils, a review, *Zeitschrift*
856 *für Pflanzenernährung und Bodenkd.*, 140(2), 159–174, doi:10.1002/jpln.19771400205, 1977.

857 Schwartz, D., Mariotti, A., Trouve, C., Van Den Borg, K. and Guillet, B.: Etude des profils
858 isotopiques 13C et 14C d'un sol ferrallitique sableux du littoral congolais : implications sur la
859 dynamique de la matière organique et l'histoire de la végétation, *Comptes Rendus l'Académie*
860 *des Sci. 2 Mécanique...*, 1992, 315, p. 1411-1417. ISSN 0249-6305, 315, 1411–1417, 1992.

861 Sitch, S., Smith, B., Prentice, I. C., Arneth, a., Bondeau, a., Cramer, W., Kaplan, J. O.,
862 Levis, S., Lucht, W., Sykes, M. T., Thonicke, K. and Venevsky, S.: Evaluation of ecosystem
863 dynamics, plant geography and terrestrial carbon cycling in the LPJ dynamic global
864 vegetation model, *Glob. Chang. Biol.*, 9(2), 161–185, doi:10.1046/j.1365-2486.2003.00569.x,
865 2003.

866 Stuiver, M. and Polach, H. A.: Reporting of 14C data, *Radiocarbon*, 19(3), 355–363,
867 doi:10.1016/j.forsciint.2010.11.013, 1977.

868 Taylor, K. E., Stouffer, R. J. and Meehl, G. a.: An overview of CMIP5 and the experiment

869 design, *Bull. Am. Meteorol. Soc.*, 93(4), 485–498, doi:10.1175/BAMS-D-11-00094.1, 2012.

870 Tisnérat-Laborde, N., Thil, F., Synal, H.-A., Hatté, C., Cersoy, S., Gauthier, C., Kaltnecker,
871 E., Massault, M., Michelot, J.-L., Noret, A., Noury, C., Siani, G., Tombret, O., Vigne, J.-D.,
872 Wacker, L. and Zazzo, A.: A new compact AMS facility measuring ¹⁴C dedicated to
873 Environment, Climate and Human Sciences, in 22nd International Radiocarbon Conference,
874 Dakar, Senegal. November 2015. Oral presentation, pp. 16–20., 2015.

875 Todd-Brown, K. E. O., Randerson, J. T., Post, W. M., Hoffman, F. M., Tarnocai, C., Schuur,
876 E. a. G. and Allison, S. D.: Causes of variation in soil carbon simulations from CMIP5 Earth
877 system models and comparison with observations, *Biogeosciences*, 10(3), 1717–1736,
878 doi:10.5194/bg-10-1717-2013, 2013.

879 Trumbore, S.: Age of Soil Organic Matter and Soil Respiration : Radiocarbon Constraints on
880 Belowground C Dynamics, *Ecol. Appl.*, 10(2), 399–411, doi:10.1890/1051-
881 0761(2000)010[0399:AOSOMA]2.0.CO;2, 2000.

882 Wieder, W. R., Bonan, G. B. and Allison, S. D.: Global soil carbon projections are improved
883 by modelling microbial processes, *Nat. Clim. Chang.*, 3(8), 1–4, doi:10.1038/nclimate1951,
884 2013.

885 WRB: World reference base for soil resources 2006: a framework for international
886 classification, correlation and communication., 2006.

887 Wynn, J. G., Bird, M. I. and Wong, V. N. L.: Rayleigh distillation and the depth profile of
888 ¹³C/¹²C ratios of soil organic carbon from soils of disparate texture in Iron Range National
889 Park, Far North Queensland, Australia, *Geochim. Cosmochim. Acta*, 69(8), 1961–1973, 2005.

890

891

892

893

894

895

896 **Table 1.** General description of the studied sites. The mean bulk density, pH and clay fraction
 897 values calculated from the different soil layers depths available from the data were used as
 898 input for each site. For the Mons and Feucherolles sites, min and max values of pH and clay
 899 fraction are provided between brackets.

Site name	Feucherolles	Mons	Kissoko	Misiones
Sampling Date	April 2011	March 2011	May 2014	May 2015
Location	France	France	Congo	Argentina
Coordinates	48.90°N, 1.97°E	49.87°N, 3.03°E	4.35°S, 11.75°E	27.65°S, 55.42°W
Elevation (m)	120	88	100	NA
Mean Annual Rainfall (mm)	660	680	1400	1850
Mean Annual Temperature (°C)	11.2	11	25	20
Soil Type (WRB)	Luvisol	Luvisol	Arenosol	Acrisol
Land Use	Temperate broad-leaved summergreen forest	Grassland	Native savanna	Tropical broad-leaved evergreen forest
Mean Bulk Density (g cm ⁻³)	1.34	1.4	1.48	1.15
Mean pH	5.9 (5.12-8.55)	6.9 (6.70-7.56)	5.2	5.2
Mean Clay Fraction (%)	20 % (13-30 %)	23 % (19-27 %)	5 %	58 %

900

901 **Table 2.** The main differences between the three simulations

	Flux from slow pool to passive pool	Turnover time of the passive pool (year)	Diffusion (m ² year ⁻¹)
Control	0.07	462	$D(z) = 1.10^{-4}$
He et al., (2016) parameterization	0.0049	6468	$D(z) = 1.10^{-4}$
Depth-varying diffusion constant	0.07	462	$D(z) = 5.42. 10^{-4} e^{(-0.04z)}$

902

903

904

905

906 **Table 3.** The correlation coefficient (r) between model outputs and measurements for carbon
 907 stock (kg C m^{-2}) over the soil profile, for the four sites. The results of the initial version of the
 908 model ORCHIDEE-SOM- ^{14}C (Control) as well as those from the version including the
 909 modification according to (He et al., 2016) (He et al., (2016) parameterization) and diffusion
 910 varying according to the depth (Depth-varying diffusion constant) are provided.
 911

		r	Mean total soil carbon (kg C m^{-2}) Model	Mean total soil carbon (kg C m^{-2}) Measurements
Misiones	Control	0.44	2.03	2.14±0.30
	He et al., (2016) parameterization	0.69	7.38	
	Depth-varying diffusion constant	0.46	2.23	
Kissoko	Control	0.14	0.76	0.42±0.38
	He et al., (2016) parameterization	0.55	2.44	
	Depth-varying diffusion constant	0.13	0.88	
Feucherolles	Control	0.20	0.70	0.66±0.08
	He et al., (2016) parameterization	0.11	2.33	
	Depth-varying diffusion constant	0.22	0.77	
Mons	Control	0.49	2.37	0.8±0.10
	He et al., (2016) parameterization	-0.14	9.99	
	Depth-varying diffusion constant	0.48	2.42	

912
 913 **Table 4.** The correlation coefficient (r) between model outputs and measurements and the
 914 mean values (provided by the model and the measurements) over the profile according to
 915 F^{14}C for the four sites. The results of the initial version of the model ORCHIDEE-SOM- ^{14}C
 916 (Control) as well as those from the version including the modification according to (He et al.,
 917 2016) (He et al., (2016) parameterization) and diffusion varying according to the depth
 918 (Depth-varying diffusion constant) are provided.
 919

		r	Mean Model	Mean Measurements
Misiones	Control	0.55	0.920	0.930±0.009
	He et al., (2016) parameterization	0.50	0.560	
	Depth-varying diffusion constant	0.60	0.900	
Kissoko	Control	0.40	0.995	0.985±0.004
	He et al., (2016) parameterization	0.30	0.620	
	Depth-varying diffusion constant	0.55	0.995	
Feucherolles	Control	0.55	0.915	0.725±0.005
	He et al., (2016) parameterization	0.55	0.550	
	Depth-varying diffusion constant	0.60	0.890	
Mons	Control	0.75	0.860	0.815±0.005
	He et al., (2016) parameterization	0.70	0.510	
	Depth-varying diffusion constant	0.80	0.835	

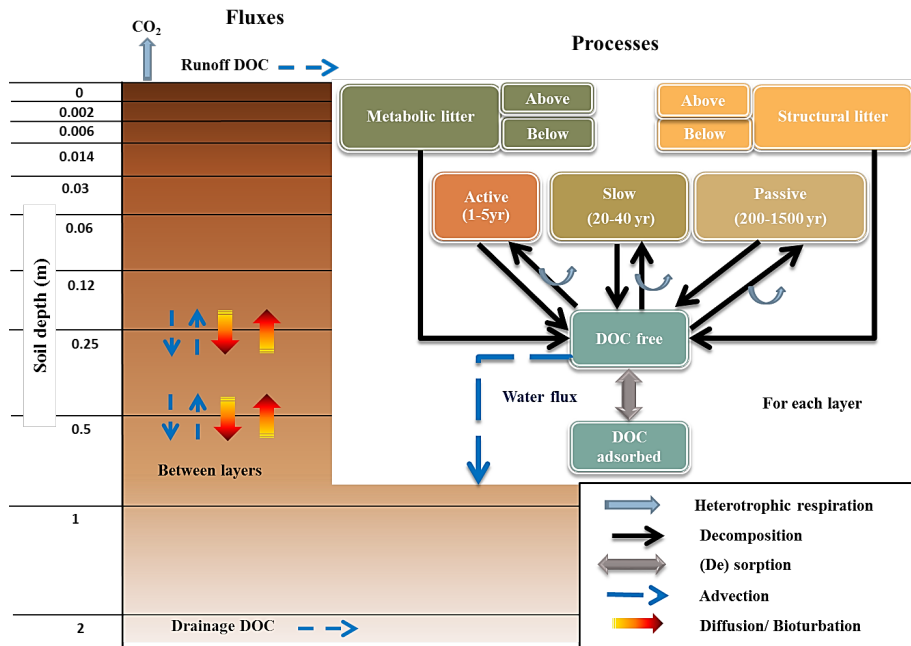
920

921 **Table 5.** F¹⁴C profile obtained for each site.

Sites	Soil depth (cm)	F ¹⁴ C
Misiones	0-5	1.08
	5-10	1.04
	10-15	1.05
	15-20	0.99
	20-30	0.99
	30-40	0.87
	40-50	0.91
	50-60	0.76
	60-80	0.79
	80-100	0.79
Kissoko	0-5	1.06
	5-10	1.07
	10-15	1.07
	15-20	1.08
	20-30	1.05
	30-40	1.04
	40-50	1.02
	50-60	0.97
	60-80	0.90
	80-100	0.81
		100-120
Feucherolles	0-2	1.08
	16-18	1.05
	40-45	0.92
	75-85	0.69
	105-115	0.54
	125-135	0.53
	147-157	0.26
Mons	0-2	1.02
	2-4	1.03
	18-20	1.03
	45-50	0.87
	60-65	0.71
	82-92	0.65
	102-112	0.64
	142-152	0.55

922

923



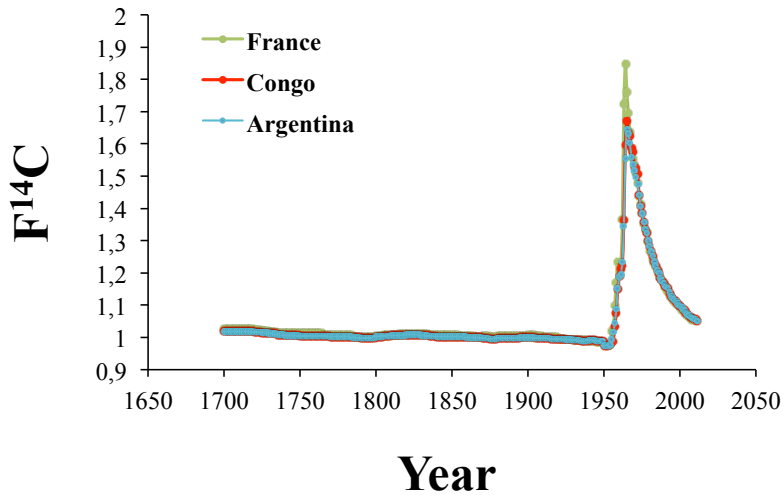
924

925

926 **Figure 1.** Overview of the different fluxes and processes in soil as presented in the version of
927 ORCHIDEE-SOM adapted from Camino-Serrano et al. (2017).

928

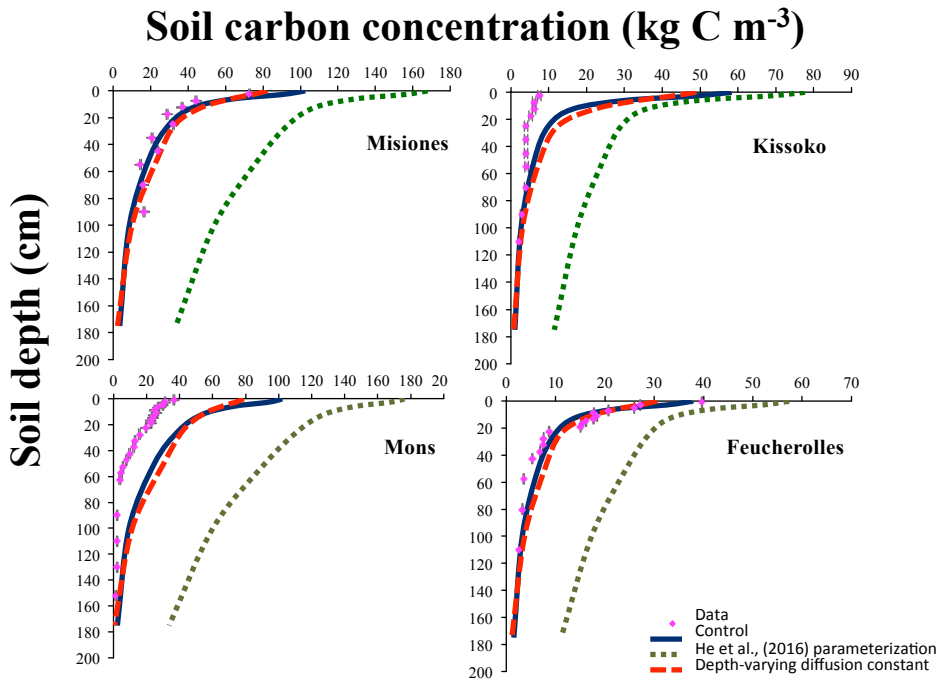
929



930

931 **Figure 2.** Evolution of the $F^{14}C$ of atmospheric CO_2 in Argentina, Congo and France (data
932 from Hua et al. 2013).

933



935

936 **Figure 3.** Total soil carbon (kg C m^{-3}) according to the depth for the four sites. The results of
 937 the initial version of the model ORCHIDEE-SOM- ^{14}C (Control) as well as those from the
 938 version including the modification according to (He et al., 2016) (He et al., (2016)
 939 parameterization) and diffusion varying according to the depth (Depth-varying diffusion
 940 constant) are shown.

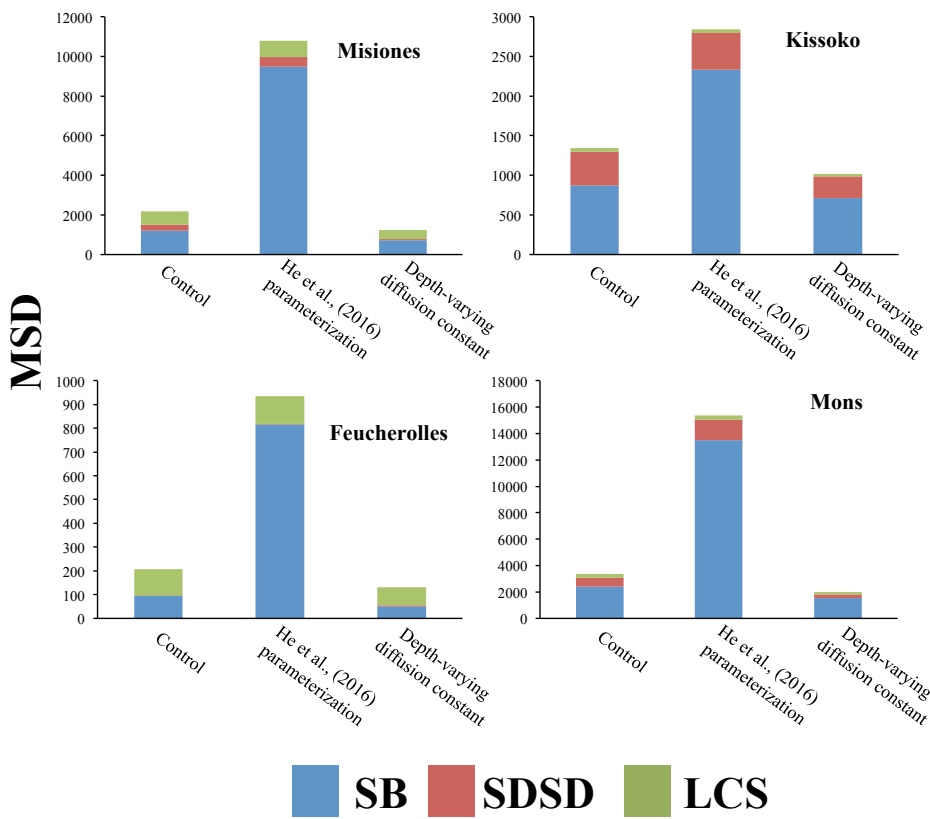
941

942

943

944

945



946

947

948

949

950

951

952

953

954

955

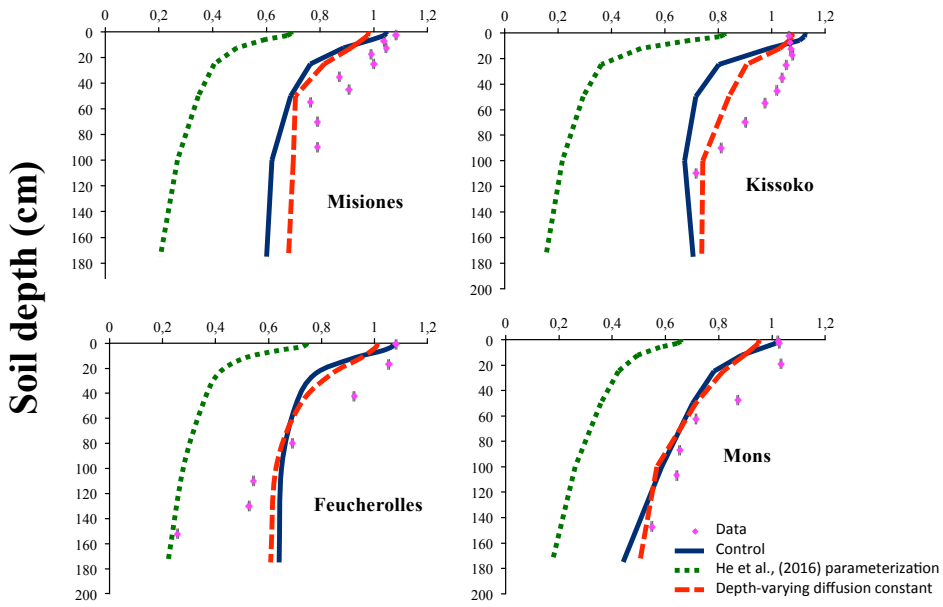
956

957

958

Figure 4. Mean Squared Deviation (MSD) and its components for total soil carbon (kg C m^{-6}): lack of correlation weighted by the standard deviation (LCS), squared difference between standard deviations (SDSD) and the squared bias (SB). For the four sites, the results of the initial version of the model ORCHIDEE-SOM- ^{14}C (Control as well as those from the version including the modification according to (He et al., 2016) (He et al., (2016) parameterization) and diffusion varying according to the depth (Depth-varying diffusion constant), are shown.

F¹⁴C



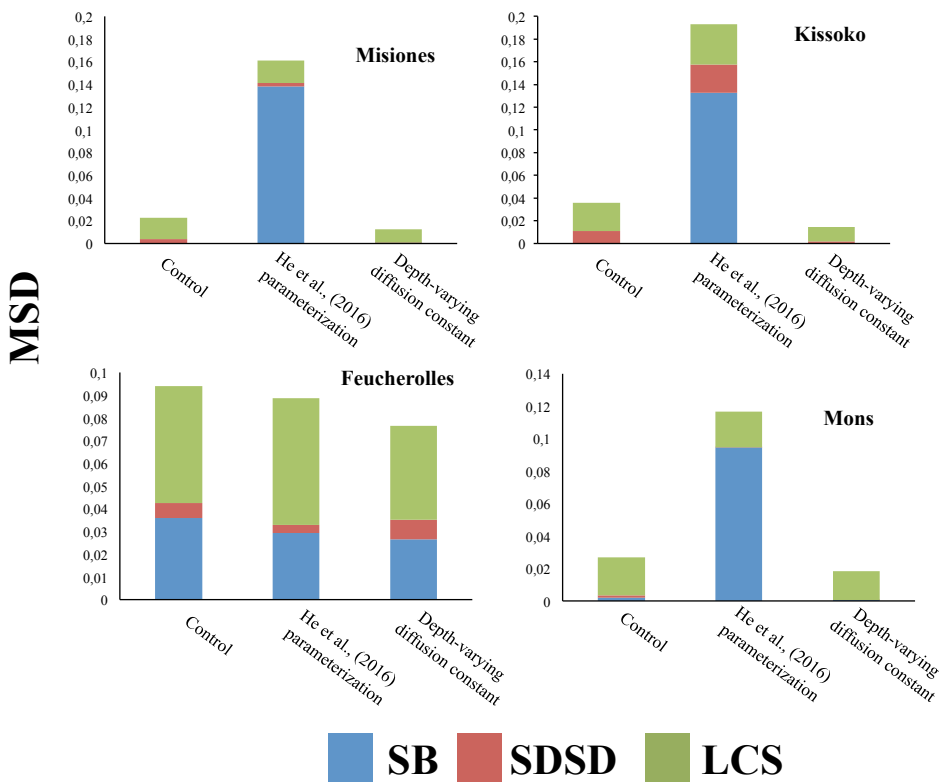
959

960 **Figure 5.** Modern fraction $F^{14}C$ according to the depth, for the four sites. The results of the
961 initial version of the model ORCHIDEE-SOM- ^{14}C (Control) as well as those from the version
962 including the modification according to He et al., (2016) (He et al., (2016) parameterization)
963 and diffusion varying according to the depth (Depth-varying diffusion constant) are shown.

964

965

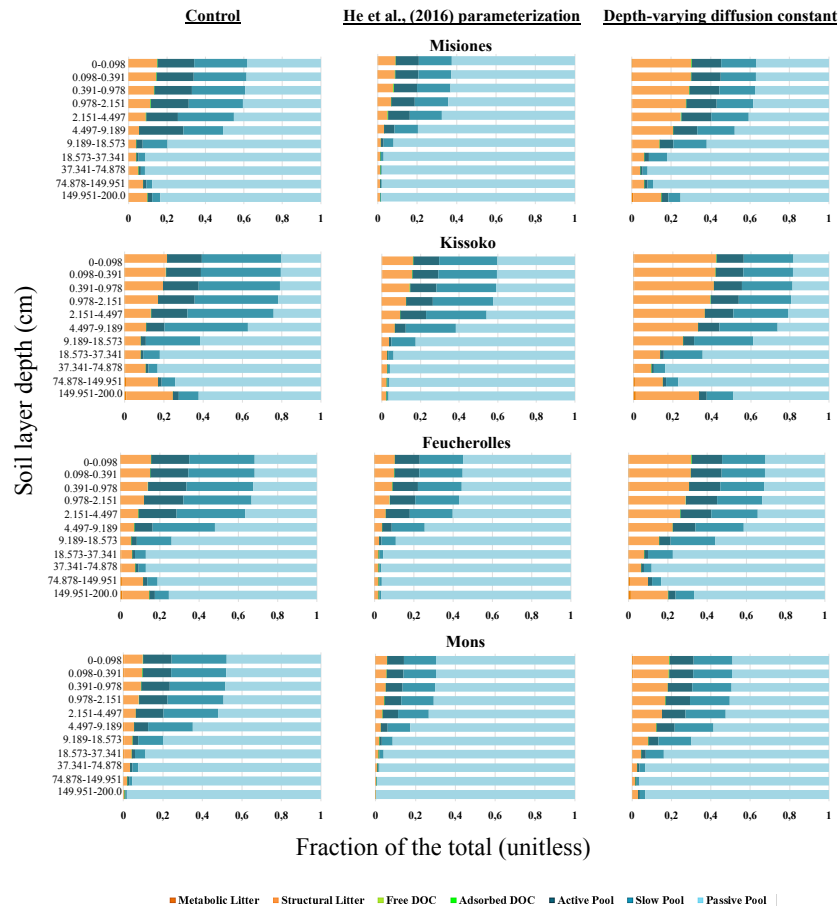
966



967
968

969 **Figure 6.** Mean Squared Deviation (MSD) and its components: lack of correlation weighted
970 by the standard deviation (LCS), squared difference between standard deviations (SDDS) and
971 the squared bias (SB) calculated for modern fraction $F^{14}C$. For the four sites, the results of the
972 initial version of the model ORCHIDEE-SOM- ^{14}C (Control) as well as those from the version
973 including the modification according to He et al., (2016) (He et al., (2016) parameterization)
974 and diffusion varying according to the depth (Depth-varying diffusion constant) are shown.

975
976



977

978 **Figure 7.** Relative proportion of each of the soil carbon pools summing the total soil carbon
 979 at each soil layer. The results of the initial version of the model ORCHIDEE-SOM-¹⁴C
 980 (Control, left pattern) as well as those from the version including the modification according
 981 to (He et al., 2016) (He et al., (2016) parameterization, pattern in the middle) and diffusion
 982 varying according to the depth (Depth-varying diffusion constant, right pattern) are shown.

983